

The Globular Cluster Mass Function as a Remnant of Violent Birth

Bruce G. Elmegreen

*IBM T. J. Watson Research Center, 1101 Kitchawan Road, Yorktown Heights, New York
10598 USA*

bge@us.ibm.com

ABSTRACT

The log-normal shape of the mass function for metal-poor halo globular clusters is proposed to result from an initial M^{-2} power law modified rapidly by evaporation, collisions with clouds, and mutual cluster interactions in the dense environment of a redshift $z \sim 5 - 15$ disk galaxy. Galaxy interactions subsequently spray these clusters into the galaxy group environment, where they fall into other growing galaxies and populate their halos. Clusters forming later in $z \sim 2 - 5$ galaxies, and those formed during major mergers, produce metal-rich globulars. Monte Carlo models of evolving cluster populations demonstrate the early formation of a log-normal mass function for typical conditions in high-redshift galaxies.

Subject headings: globular clusters: general — galaxies: formation — galaxies: starburst — stars: formation

1. Introduction

The globular cluster mass function (GCMF) in present-day galaxy halos is approximately log-normal with a peak $M_p \sim 10^{5.3} M_\odot$ (see reviews in McLaughlin 2003; Brodie & Strader 2006). The origin of this peaked distribution is not understood. Wherever massive dense clusters like globular clusters (GCs) are formed today, they have a power-law mass function like $dN/dM \propto M^{-2}$, or a Schechter function with a similar power law at low mass and a cutoff at high mass (see review in Gieles 2009). Consequently, one theory for halo GCs is that they begin with a power-law mass function and then lose their low-mass members through dispersal over a Hubble time (Fall & Rees 1977; Okazaki & Tosa 1995; Elmegreen & Efremov 1997; Fall & Zhang 2001). The dispersal rate works out about right if the disruption process is thermal evaporation (McLaughlin & Fall 2008).

The problem with this model is that the GCMF does not vary with radius in several nearby galaxies (Tamura et al. 2006; Jordán et al. 2007), and evaporation is expected to occur faster in the inner regions where tidal forces are larger, thereby shifting the peak toward higher masses there. A model in which GCs have a small range of pericenters can fix this problem (Fall & Zhang 2001), but the resulting GC velocities disagree with observations in M87 (Vesperini et al. 2003).

What is expected to drive the radial gradient in evaporation rate is a gradient in the tidal density (Gieles & Baumgardt 2008), which is the average GC density inside the GC tidal radius. This tidal density is difficult to observe directly and is not necessarily proportional to the average density inside the half-light radius, which is observed directly. The half-light density does not correlate well with radial distance. Noting this, Chandar, Fall & McLaughlin (2007) and McLaughlin & Fall (2008) fit the GCMFs in M104 and the Milky Way to evolved Schechter functions for three bins of half-light density using GC evaporation rates proportional to the square roots of these densities. The results are consistent with faster evaporation, i.e., higher peak mass, at greater half-light density, regardless of galactocentric radius. McLaughlin & Fall (2008) also fit the Milky Way GCMF for three bins of tidal density using evaporation rates given by that density.

An alternative model is that GCs are born with a peaked mass function and then keep it over a Hubble time (Vesperini et al. 2003; Parmentier & Gilmore 2005). Log-normal mass functions evolve somewhat self-similarly during evaporation, and their peak mass and width may even converge to the observed values (Vesperini 1998). The peak mass would also be uniform with galactocentric radius after a while. Initially peaked GCMFs could result from a lack of low-mass clouds in the early GC environment (Parmentier & Gilmore 2007). Another model considers variable star formation efficiencies with a greater probability for lower cluster masses to disperse when the gas leaves (Parmentier et al. 2008; Baumgardt, Kroupa & Parmentier 2008). A third model is that low mass clusters were born with lower central concentrations and so evaporated more quickly than high mass clusters (Vesperini & Zepf 2003). There is no direct evidence for any of these models because all known clusters today are born with power-law mass functions. For one of these models to be viable, the qualitative nature of cluster formation would have to be different in the early Universe.

We consider here a model where halo GCs form with power-law mass functions that are quickly converted into peaked functions in very dense cloudy environments. The GCMF stays peaked and insensitive to environment thereafter (Vesperini 1998). This model involves the same physical process of cluster formation that is present today, i.e., gravitational collapse in giant gas complexes, and the cluster-forming cloud-cores are probably similar as well,

considering that GC densities, masses, and IMFs are not unusual. What differed in young galaxies was a much denser and more turbulent interstellar medium (ISM) than we have in main galaxy disks today (Förster Schreiber et al. 2006; Genzel et al. 2006; Law et al. 2007). GC formation in $z > 10$ dwarf galaxies was discussed by Bromm (2004); bulge-GC formation in $z \sim 2$ galaxy clumps was discussed by Shapiro, Genzel & Förster Schreiber (2010), and simulations of GC formation in young galaxy disks were made by Kravtsov & Gnedin (2005). The main point here is that when the density is high and the motions are fast, clusters should frequently collide with cloud clumps and other clusters during their first several hundred Myrs. These collisions destroy the lowest mass clusters and produce a log-normal GCMF.

2. Collisional Dispersal of Clusters in High Density Environments

Clusters heat up or disperse completely when their potential energy changes quickly. This can result from rapid gas expulsion or from collisions with dense clouds and other clusters. In a star-forming environment, there are many opportunities for collisions. The cluster dispersal rate therefore starts high after birth, and it decreases as the star-forming cloud dissipates and all the clusters and dense cores drift away. We have studied time-dependent cluster collisions elsewhere (Elmegreen & Hunter 2010). Here we consider a time-average collision rate and ask what it has to be in order to convert a power-law initial cluster mass function into a peaked mass function during the starburst phase of a young galaxy.

The collisional disruption rate is taken from Gieles et al. (2006), who use a cluster evolution equation $dM/dt = -M/t_{\text{dis}}$ with a disruption time

$$t_{\text{dis}} = 37 \frac{M^{0.61}}{\Sigma_n \rho_n} \text{ Myr}; \quad (1)$$

Σ_n is the average column density of a collision partner, in $M_\odot \text{ pc}^{-2}$, ρ_n is the average density of collision partners in the neighborhood, in $M_\odot \text{ pc}^{-3}$, and M is the cluster mass. Gieles et al. use $\Sigma_n = 170 M_\odot \text{ pc}^{-2}$ for typical GMCs and $\rho_n = 0.03 M_\odot \text{ pc}^{-3}$ for the ambient ISM. Then $\Sigma_n \rho_n \sim 5.1 M_\odot^2 \text{ pc}^{-5}$ and $t_{\text{dis}} \sim 7.3 M^{0.61} \text{ Myr}$, which is 8.2 Gyr for $M = 10^5 M_\odot$.

The disruption time is less at higher density. If we require disruption of $M < 10^5 M_\odot$ clusters within the time span of the gas-rich phase of a young galaxy disk, which may be 500 Myr (e.g., Tacconi et al. 2008), then $t_{\text{dis}} = 500 \text{ Myr}$ and $\Sigma_n \rho_n \sim 80 M_\odot^2 \text{ pc}^{-5}$ – a factor of 16 larger than the local ISM value used by Gieles et al.. This factor may be accounted for by a higher average density in the cluster environment and a higher average column density for likely collision partners. For example, ρ_n could be ~ 10 times higher in a galaxy with 50% of the disk mass in the form of clumpy gas (Tacconi et al. 2010), and Σ_n could be

$\sim 10^3 M_\odot \text{ pc}^{-2}$ or more for massive molecular cores and other clusters. If we require that t_{dis} equals 10 times the dynamical time of the ISM, which is $10/(G\rho_n)^{0.5}$, then $\Sigma_n \rho_n^{0.5}$ has to equal $280 M_\odot^{1.5} \text{ pc}^{-3.5}$ for $M = 10^5 M_\odot$. Even this is reasonable for an extremely gas-rich and dense disk where ρ_n might be $\sim 1 M_\odot \text{ pc}^{-3}$ ($\sim 30 \text{ atoms cm}^{-3}$) in regions one kpc in size. The clumpy galaxies observed at $z \sim 2$ are a good example of such an environment (Elmegreen et al. 2009). The ISM density should be even larger at $z \sim 5 - 15$, where many halo GCs are likely to have formed. Young galaxies are denser than today’s galaxies because the Universe was denser, by the factor $(1+z)^3 \sim 1000$ for the redshift of interest here. Young galaxies are also smaller than today’s galaxies (Oesch et al. 2010) and either represent the inner (dense) parts of today’s galaxies or separate objects that merged into dense spheroids over time.

2.1. Monte Carlo Simulations with Constant Cluster Birthrate

The time evolution of cluster populations was determined for Monte Carlo simulations with constant cluster birthrates and cluster disruption rates given by

$$dM/dt = -M/t_{\text{dis}} \ ; \ t_{\text{dis}} = \xi M^\gamma; \quad (2)$$

$\xi = 37/(\Sigma_n \rho_n)$ could be ~ 0.01 or smaller for units of column density in $M_\odot \text{ pc}^{-2}$ and density in $M_\odot \text{ pc}^{-3}$. In the Gieles et al. (2006) model, $\gamma \sim 0.6$; we take $\gamma = 0.62$ to be consistent with the evaporation model in Lamers et al. (2005). We also ran simulations with $\gamma = 1$, which is appropriate for Spitzer (1987) evaporation and for Spitzer (1958) collisional disruption with a weak mass-radius relation, as observed by Bastian et al. (2005) and others. That is, Gieles et al. (2006) and Spitzer (1958) both derived $t_{\text{dis}} \propto \rho_{\text{cl}}/(\Sigma_n \rho_n)$ for collisional disruption with cluster internal density ρ_{cl} . Bastian et al. used $\rho_{\text{cl}} \propto M^{0.61}$, but it is also possible that $\rho_{\text{cl}} \propto M$. Both collisional disruption and cluster evaporation should be rapid in the high density environments of young GCs. Collisional disruption probably dominates evaporation in the disk environment (Gieles et al. 2006).

Values of ξ that give a mass distribution peak M_p when the cluster population has an age T may be determined from the relation $\xi M_p^\gamma = T$. For $T = 1000 \text{ Myr}$ and $M_p = 10^5 M_\odot$, $\xi = 0.01$ when $\gamma = 1$, and $\xi = 0.79$ when $\gamma = 0.62$. These ξ are reasonable for starburst conditions in young, dense galaxies.

In the simulations, clusters masses were randomly chosen from an initial $dn/dM \propto M^{-2}$ mass function that extends from a minimum mass $M_{\text{min}} = 10 M_\odot$ to a maximum mass of $10^8 M_\odot$. The cluster formation rate is one cluster per time step, dt , measured in Myr. At each time step, equation (2) is applied to every cluster, and every cluster mass is reduced

accordingly. Clusters with masses dropping below $0.1M_{\min}$ are not followed. The results after 10 Gyr are shown on a plot of $\log M$ versus $\log T$ for each current cluster mass M and age T (Fig. 1). The age is defined to be the current time in the simulation minus the time of formation of the cluster. We are interested in the distribution of cluster mass at an age of ~ 500 Myr or so, when the starburst ends and the clusters begin to scatter. This distribution can be read off the plot at $T = 500$ Myr. The plot extends to $T = 10$ Gyr for comparison.

Figure 1 shows $\log M - \log T$ distributions of cluster populations for various values of ξ and for $\gamma = 0.62$ on the left and $\gamma = 1$ on the right. All of the distributions have about the same form with more or less attrition over age in cases with low or high ξ , respectively. The upper envelope of the cluster mass comes from the size-of-sample effect, which states that the most massive cluster in an $dn/dM \sim M^{-2}$ distribution is directly proportional to the number of clusters in the sample. This maximum increases linearly with T on a plot like this because the time interval ΔT increases linearly with T for equal intervals in $\log T$. The lower envelope of the distributions increase as $M \propto T^{1/\gamma}$ because that is the mass at which $t_{\text{dis}} = T$. The dashed green line is $M_{\min} = 10 M_{\odot}$. For $\gamma = 1$, the upper and lower envelopes are parallel so the mass range of the mass function at any one age remains about constant. For $\gamma = 0.62$, the bottom envelope increases faster than the top envelope. Two cluster formation rates ($1/dt$) are used to give good numbers of points at different ξ .

Lower ξ makes the characteristic mass of the clusters higher for a given age. Figure 1 has vertical and horizontal dotted lines at fiducial markers $T = 1000$ Myr and $M = 10^5 M_{\odot}$. At $T = 1000$ Myr with $\gamma = 0.62$, $\xi = 0.1$ has a mass distribution centered slightly higher than $M \sim 10^5 M_{\odot}$, while $\xi = 1$ has a mass distribution centered slightly lower than this. The value $\xi = 0.5$ gives a mass at the peak of the function $M_p \sim 10^5 M_{\odot}$, as predicted approximately above. For $\gamma = 1$, a value of $\xi \sim 0.01$ gives this M_p at $T = 1000$ Myr, as also predicted.

Figure 2 shows log-normal fits to the cluster mass functions versus cluster age in four age intervals, $\log T = 2 - 2.5$, $2.5 - 3$, $3 - 3.5$, and $3.5 - 4$ for T in Myr. The trend of increasing mean $\log M$ with increasing age (Figure 1) is evident in Figure 2. The scatter in the diagram is from the small numbers of clusters in the age intervals (50 to 500, depending on ξ and γ). The solutions give the desired $M_p \sim 10^5$ when $T \sim 10^3$ Myr if ξ is small.

2.2. Monte Carlo Simulations with Cluster Birth for 500 Myr

Figure 3 shows another case. The blue dots come from previous models (Figure 1). The red crosses are for a model where cluster formation occurs for the first 500 Myr and cluster

disruption uses equation (2), but then star formation stops and the disruption rate decreases in proportion to the remaining cluster mass as

$$dM/dt = - \left(\frac{M_{\text{tot}}(t > 500 \text{ Myr})}{M_{\text{tot}}(t = 500 \text{ Myr})} \right) \frac{M}{t_{\text{dis}}} \quad (3)$$

for times between 500 Myr and 1000 Myr. This model simulates normal cluster formation and disruption during 500 Myr when dense gas is present, followed by no cluster formation and diminished disruption for another 500 Myr after the gas disperses. Only the log-normal GCMF remains; fits are shown in Figure 4. Figure 2 shows black symbols for the peak masses and dispersions in this second model at $T = 2.75 - 3.25$ Myr; they should be compared with the black curves, which have the same γ and ξ .

3. Discussion

We propose that old halo GCs formed by normal processes much like clusters form today, but that all of these processes occurred in young galaxies at very high densities, higher than today’s ISM densities by factors of 10 to 100. Then collisional disruption and evaporation was rapid enough to produce a peaked mass function in the young galaxy. Subsequent evolution by evaporation in lower density environments preserved this function, although slight changes in peak mass and width probably occurred.

Given this basic model, there are many possibilities for the delivery of these clusters into modern galaxies. The dense galaxies they formed in are most likely not the same as the galaxies or inner parts of the galaxies that currently host them. Their presence in galaxy halos today implies that they were delivered to the host in a non-dissipative way, perhaps by infall along with most of the host’s other baryons. For example, the oldest GCs could have formed in small dense galaxies that formed as condensations in larger-scale cold gas flows. The cold flows make today’s spiral disks (Dekel et al. 2009; Agertz, Teyssier & Moore 2009; Keres et al. 2009), and the GCs along with other condensations in the flow populate modern halos. The small dense galaxies could also have collided before they entered the modern galaxy’s potential well, freeing up the GCs which would then enter the well as free-floaters along with the other material. Some small galaxies are still adding GCs to modern halos (e.g., Carraro et al. 2007; Gao et al. 2007; Casetti-Dinescu 2009; Smith et al. 2009). The oldest GC populations in elliptical galaxies presumably formed in small dense galaxies and fell into spiral halos too in the same way, but then ended up in ellipticals after major mergers of the spirals. These oldest GCs would be the blue, metal-poor populations in spiral and elliptical halos. GCs formed during major mergers would be redder and more metal-rich (Brodie & Strader 2006).

The uniform properties of old halo globular clusters (color, density, IMF, peak GCMF mass, metallicity) follow from this model if we postulate that GCs are the first examples of star formation at high enough metallicity to make a normal IMF. Then stellar evolution will not remove excessive amounts of gas and cause the cluster to come unbound. Top-heavy IMFs, such as those thought to produce the carbon-enhanced metal-poor stars (Tumlinson 2007; Komiya et al. 2009), lose too high a fraction of their mass during stellar evolution to keep a cluster bound. Boundedness would require them to occupy the nuclei of small galaxies so they can retain their stellar wind material in the galactic potential well. Then contamination from subsequent generations of stars would also enrich them (e.g., Marcolini et al. 2007; Bailin & Harris 2009). For clusters born in small dense disks, the uniformity of both the clusters and the GCMFs suggest that the first epoch of normal IMFs occurred when galaxies were still small and dense, and this was long before today’s spirals were assembled.

The bulge GCs of modern spirals could have a similar origin as the halo GCs, but there is no similar constraint on the constancy of their GCMFs over a range of galactocentric radii. Also, the bulge GCs formed in metal-rich environments and they are now located deep in the potential wells of their current hosts. Thus they need not have formed in separate small galaxies. They could have formed in their hosts and settled to the center after energy dissipation. This is the model by Shapiro, Genzel & Förster Schreiber (2010). They proposed that bulge GCs formed in the dense clumps of young massive $z \sim 2$ galaxies, much like we propose that metal-poor GCs formed in the dense clumps of young and small $z \sim 5 - 15$ galaxies. The local environment is about the same for each, namely high-density clumpy gas, so collisional disruption would have occurred quickly for the Shapiro et al. model too. The densities in the massive clumps of $z \sim 2$ spirals are not expected to have been as high as the densities in the disk clumps of smaller galaxies at higher redshift, however. Thus collisional disruption of low mass GCs may not have been as rapid for the Shapiro et al. model.

Our model accounts for the number of halo GCs today if a high fraction of early star formation made bound clusters. Such a high fraction is expected when the ISM pressure and velocity dispersion are large (Elmegreen 2008). The space density of GCs today is $\sim 8 \text{ Mpc}^{-3}$ (Portegies Zwart & McMillan 2000). There could have been a factor of ~ 2 more when they formed, considering evaporation (Vesperini 1998), but blue halo GCs are only half of the total. The co-moving space density of clumpy galaxies at $z \sim 1 - 2$ is $n_g \sim 2 \times 10^{-3} \text{ Mpc}^{-3}$ (Elmegreen et al. 2007). Each galaxy has ~ 5 clumps of stellar mass $\sim 10^8 M_\odot$, which would be $N_c \sim 5 \times 10^3$ clusters of mass $\sim 10^5 M_\odot$ each. Thus the space density of massive clusters would have been $n_g N_c \sim 10 \text{ Mpc}^{-3}$, with a factor-of-3 uncertainty either way. Shapiro et al. (2010) got the same result a different way. If metal-poor GCs formed in younger, smaller galaxies, then the M_{gal}^{-2} cosmological galaxy mass function means that each log interval of

galaxy mass contains the same total mass. Thus we would get these same ~ 10 GC per Mpc^3 for GC formation in galaxies 10 or 100 times less massive at higher redshifts.

Modern examples of this model may occur in dense galactic nuclear regions where we predict a rapid destruction of low mass clusters because of heightened collision and evaporation rates.

Acknowledgements: I am grateful to Enrico Vesperini and Tanuka Chattopadhyay for discussions about the GCMF, and to Dean McLaughlin for comments on the manuscript.

REFERENCES

- Agertz, O., Teyssier, R., Moore, B. 2009, *MNRAS*, 397, L64
- Bailin, J., & Harris, W.E. 2009, *ApJ*, 695, 1082
- Bastian, N., Gieles, M., Lamers, H. J. G. L. M., Scheepmaker, R. A., & de Grijs, R. 2005, *A&A*, 431, 905
- Baumgardt, H., Kroupa, P., & Parmentier, G. 2008, *MNRAS*, 384, 1231
- Brodie, J.P., & Strader, J. 2006, *ARA&A*, 44, 193
- Bromm, V. 2004, *ASPC*, 322, 499
- Carraro, G., Zinn, R., & Moni Bidin, C. 2007, *A&A*, 466, 181
- Casetti-Dinescu, D.I. et al. 2009, *ApJ*, 701, L29
- Chandar, R., Fall, S. M., & McLaughlin, D.E. 2007, *ApJ*, 668, L119
- Dekel, A., Sari, R., & Ceverino, D. 2009, *ApJ*, 703, 785
- Elmegreen, B.G. 2008, *ApJ*, 672, 1006
- Elmegreen, B.G., & Efremov, Y.N. 1997, *ApJ*, 480, 235
- Elmegreen, B.G., Elmegreen, D.M. Ravindranath, S., Coe, D.A. 2007, *ApJ*, 658, 763
- Elmegreen, B.G., Elmegreen, D.M., Fernandez, M.X., & Lemonias, J.J., 2009, *ApJ*, 692, 12
- Elmegreen, B.G., & Hunter, D.A. 2010, *ApJ*, 712, 604
- Fall, S.M., & Rees, M.J. 1977, *MNRAS*, 181, 37

- Fall, S.M., & Zhang, Q. 2001, *ApJ*, 561, 751
- Förster Schreiber, N. M. et al. 2006, *ApJ*, 645, 1062
- Gao, S., Jiang, B.-W., & Zhao, Y.-H. 2007, *ChJAA*, 7, 111
- Genzel, R. et al. 2006, *Nature*, 442, 786
- Gieles, M. 2009, *MNRAS*, 394, 2113
- Gieles, M., Portegies Zwart, S. F., Baumgardt, H., Athanassoula, E., Lamers, H. J. G. L. M., Sipior, M., & Leenaarts, J. 2006, *MNRAS*, 371, 793
- Gieles, M., & Baumgardt, H. 2008, *MNRAS*, 389, L28
- Jordan, A., McLaughlin, D.E., Côté, P., Ferrarese, L., Peng, E.W., Mei, S., Villegas, D., Merritt, D., Tonry, J.L., & West, M.J. 2007, *ApJS*, 171, 101
- Keres, D., Katz, N., Fardal, M., Davé, R., & Weinberg, D. H. 2009, *MNRAS*, 395, 160
- Komiya, Y., Suda, T., Fujimoto, M.Y. 2009, *ApJ*, 694, 1577
- Kravtsov, A.V., & Gnedin, O.Y. 2005, *ApJ*, 623, 650
- Lamers, H.J.G.L.M., Gieles, M., Bastian, N., Baumgardt, H., Kharchenko, N.V., & Portegies Zwart, S. 2005, *A&A*, 441, 117
- Law D. R., Steidel C. C., Erb D. K., Larkin J. E., Pettini M., Shapley A. E., & Wright S. A., 2007, *ApJ*, 669, 929
- Marcolini, A., Sollima, A., D’Ercole, A., Gibson, B. K., Ferraro, F. R. 2007, *MNRAS*, 382, 443
- McLaughlin, D.E. 2003, in *Extragalactic Globular Cluster Systems*, ESO Astrophysics Symposia, ed. M. Kissler-Patig. Berlin: Springer-Verlag, p. 329
- McLaughlin, D. E., & Fall, S. M. 2008, *ApJ*, 679, 1272
- Okazaki, T., & Tosa, M. 1995, *MNRAS*, 274, 48
- Oesch, P. A., Bouwens, R. J., Carollo, C. M., Illingworth, G. D., Trenti, M., Stiavelli, M., Magee, D., Labbé, I., & Franx, M. 2010, *ApJ*, 709, L21
- Parmentier, G., & Gilmore, G. 2005, *MNRAS*, 363, 326

- Parmentier, G., & Gilmore, G. 2007, MNRAS, 377, 352
- Parmentier, G., Goodwin, S. P., Kroupa, P., & Baumgardt, H. 2008, ApJ, 678, 347
- Portegies Zwart, S. F., & McMillan, S. L. W. 2000, ApJ, 528, L17
- Smith, M. C., Evans, N. W., Belokurov, V., Hewett, P. C., Bramich, D. M., Gilmore, G., Irwin, M. J., Vidrih, S., & Zucker, D. B. 2009, MNRAS, 399, 1223
- Spitzer, L., Jr. 1958, ApJ, 127, 17
- Spitzer, L., Jr. 1987, Dynamical Evolution of Globular Clusters (Princeton: Princeton University Press).
- Shapiro, K.L., Genzel, R., & Förster Schreiber, N.M. 2010, MNRAS, in press
- Tacconi, L.J. et al. 2008, ApJ, 680, 246
- Tacconi, L.J. et al. 2010, Nature, 463, 781
- Tamura, N., Sharples, R.M., Arimoto, N., Onodera, M., Ohta, K., & Yamada, Y. 2006, MNRAS, 373, 588
- Tumlinson, J. 2007, ApJ, 665, 1361
- Vesperini, E. 1998, MNRAS, 299, 1019
- Vesperini, E., & Zepf, S. E. 2003, ApJ, 587, L97
- Vesperini, E., Zepf, S. E., Kundu, A., & Ashman, K. M. 2003, ApJ, 593, 760

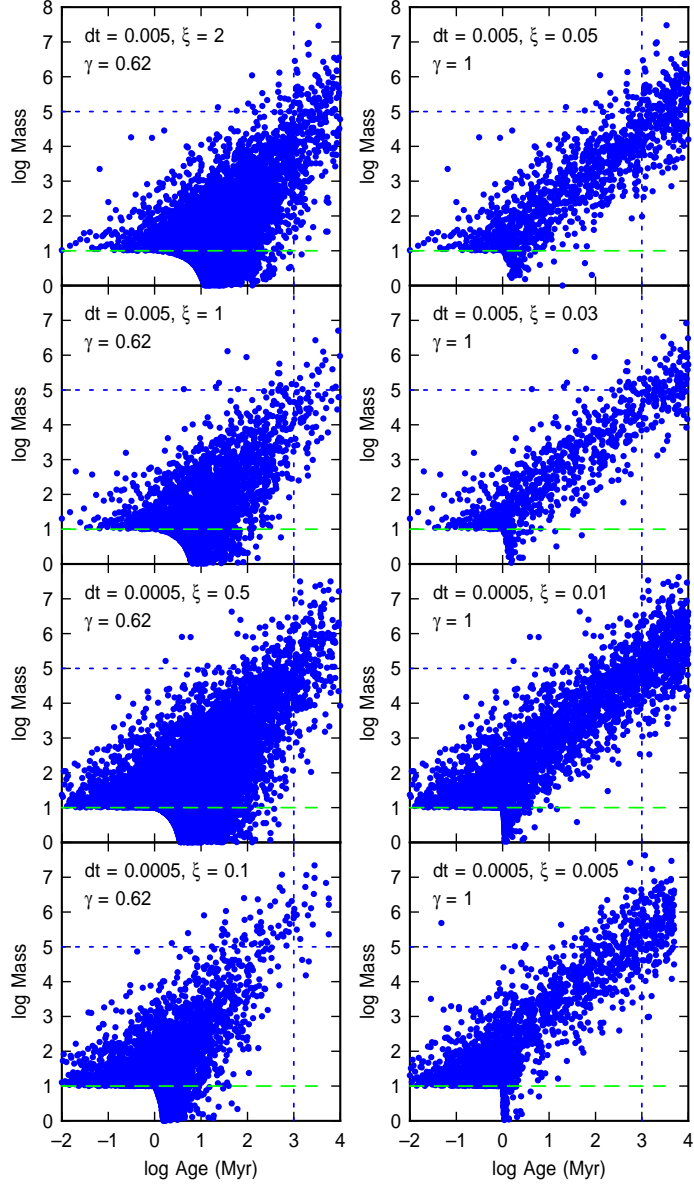


Fig. 1.— Distribution of cluster masses M and ages T after 10^4 Myr of evolution with continuous cluster formation in an $M^{-2}dM$ mass function and continuous disruption or evaporation according to equation (2) with values of γ and ξ indicated. The star formation rate is $1/dt$ for model time step dt in Myr. The horizontal dashed line is the lower limit to the mass of a formed cluster; clusters get lower mass over time because of the assumed disruption. The blue dotted lines indicate fiducial markers for age and mass where we expect a GC population should be after the starburst phase of a young galaxy. The clusters are presumed to be scattered after ~ 1 Gyr and then they evolve mostly by slow evaporation in the halos and bulges of these and other galaxies.

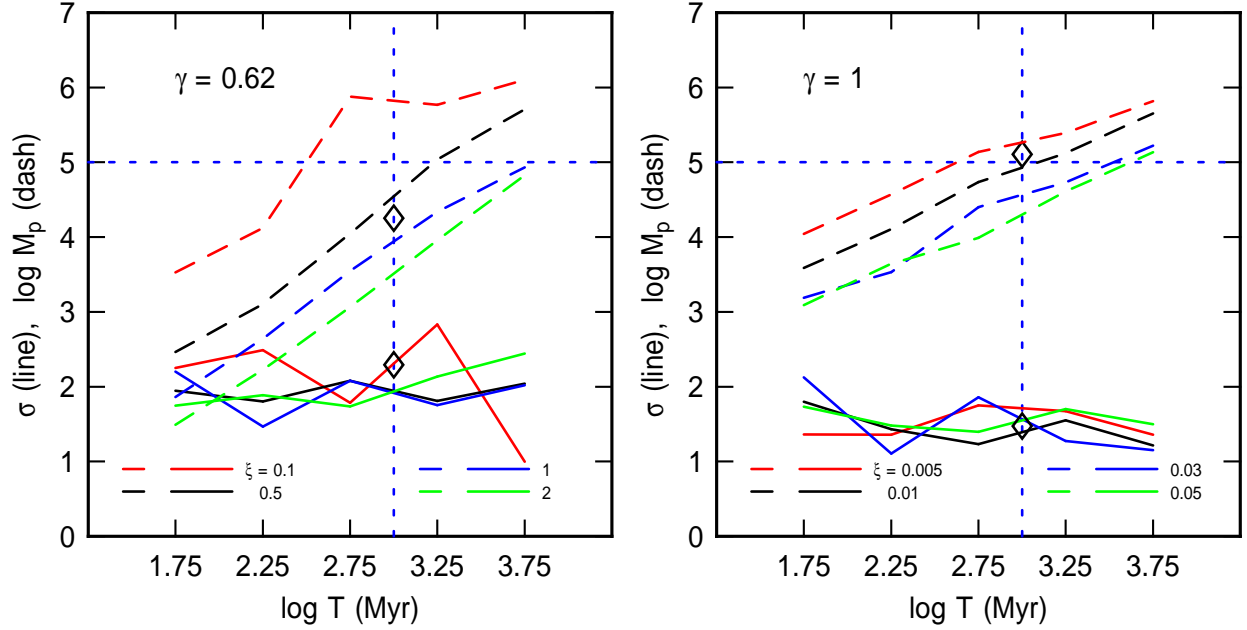


Fig. 2.— Fits for peak masses M_p and dispersions σ of log-normal cluster mass functions for 0.5 log-age intervals. Different curves are for different ξ , which is the coefficient in equation (2) for the dispersal time. The peak mass increases with age because of preferential dispersal of low mass clusters. Strong cluster disruption, corresponding to small values of ξ , can produce a peaked GCMF with $M_p \sim 10^5 M_\odot$ after ~ 1 Gyr, as indicated by the dotted lines. Diamonds give M_p and σ values for the models shown as red crosses in Fig. 3.

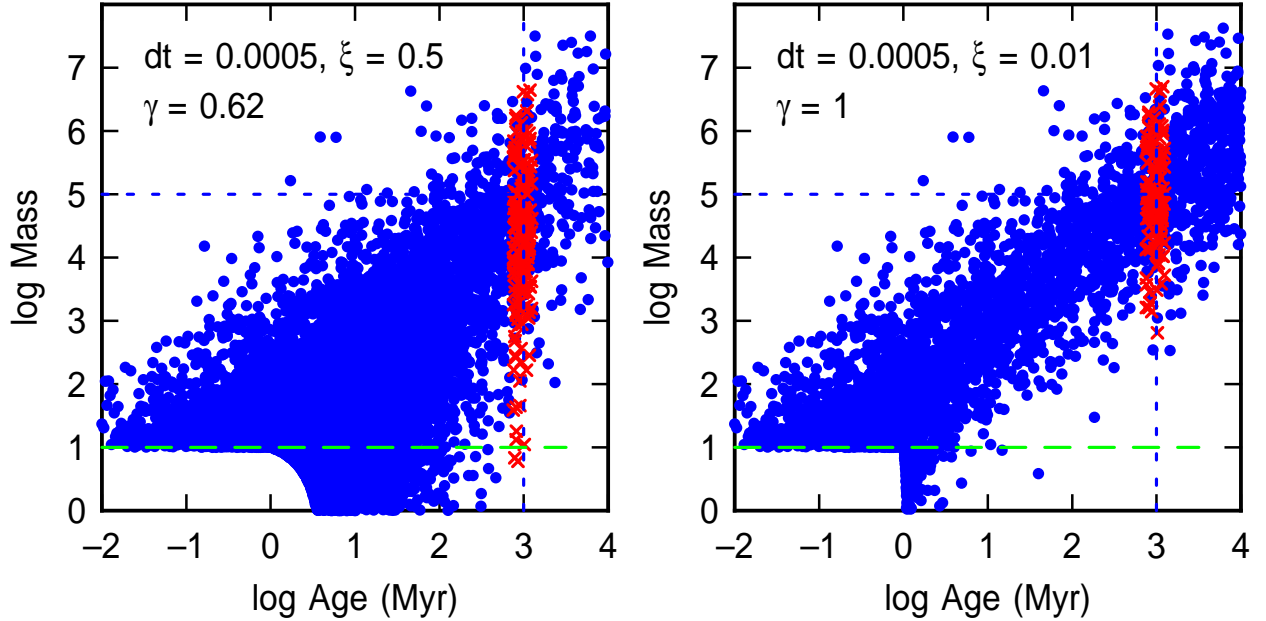


Fig. 3.— Masses and ages of cluster populations after 10^4 Myr with continuous cluster formation and dispersal (blue dots, as in Figure 1). Surviving clusters (red crosses) for a second model in which cluster formation and full-rate disruption end after 500 Myr, and then cluster disruption diminishes in proportion to the total mass of the remaining clusters. This second model is viewed after 10^3 Myr. It represents a case where clusters are formed and disrupted during a Gyr time span in a small dense galaxy at high redshift. The clusters end this phase with a log-normal mass function and presumably scatter into other forming galaxies over time, preserving this mass function.

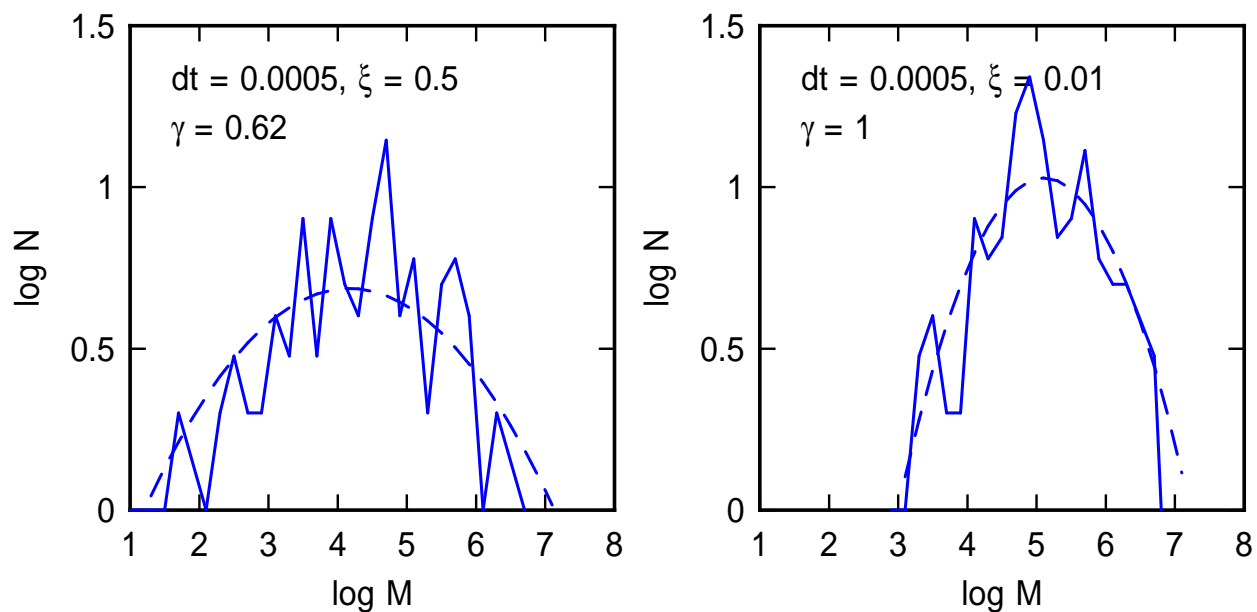


Fig. 4.— Mass distribution functions of the red crosses shown in Figure 3, along with log-normal fits. The $\gamma = 0.62$ case has a tail of low mass clusters for the assumed epoch (1 Gyr) and disruption rate (ξ), but both are reasonably peaked at around $M_p \sim 10^5 M_\odot$, making this process viable as a mechanism to inject GCs with this “initial” mass function into the converging flows of the early universe.